Supporting Information

Coupling Interface Construction of $Ni(OH)_2/MoS_2$ Composite Electrode for Efficient Alkaline Oxygen Evolution Reaction.

Ge Liu[1], Xuezhi Ouyang[1], Xue-Ling Wei[2*], Wei-Wei Bao[2], Xiao-Hua Feng[1], Jun-Jun Zhang[1,3*]

[1]School of Materials Science and Chemical Engineering, Xi'an Technological University, Xi'an, Shaanxi 710021, China.

[2]National & Local Joint Engineering Laboratory for Slag Comprehensive Utilization and Environmental Technology, School of Material Science and Engineering, Shaanxi University of Technology, Hanzhong 723000, Shaanxi, China

[3]State Key Laboratory of High-efficiency Utilization of Coal and Green Chemical Engineering, College of Chemistry & Chemical Engineering, Ningxia University, Yinchuan 750021, Ningxia, China

Correspondence to:

E-mail: weixueling@snut.edu.cn (X. L.Wei);zhangjunjun@xatu.edu.cn (J. J. Zhang).

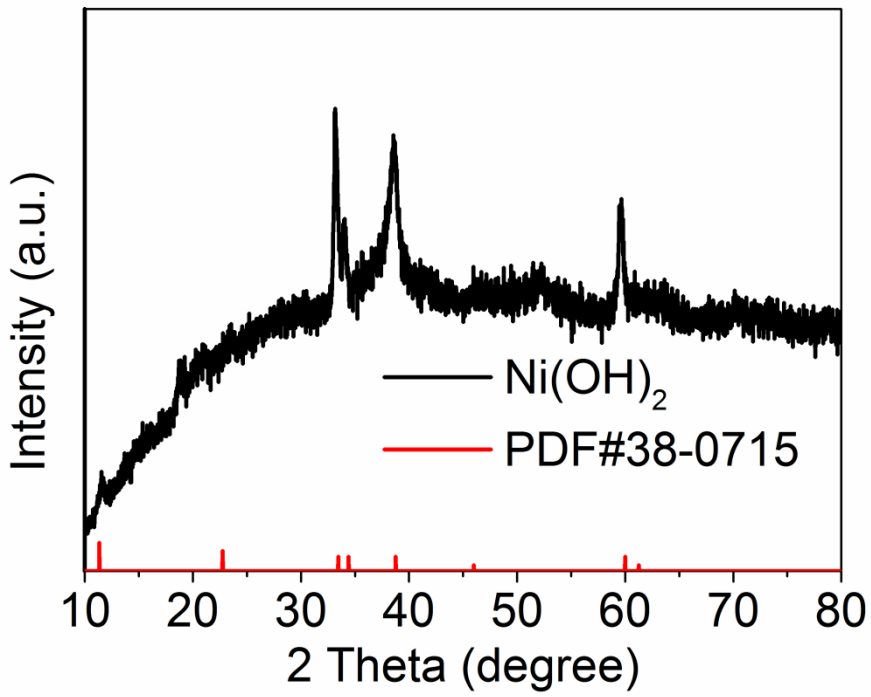

Figure S1. The XRD pattern of $Ni(OH)_2$ powder.

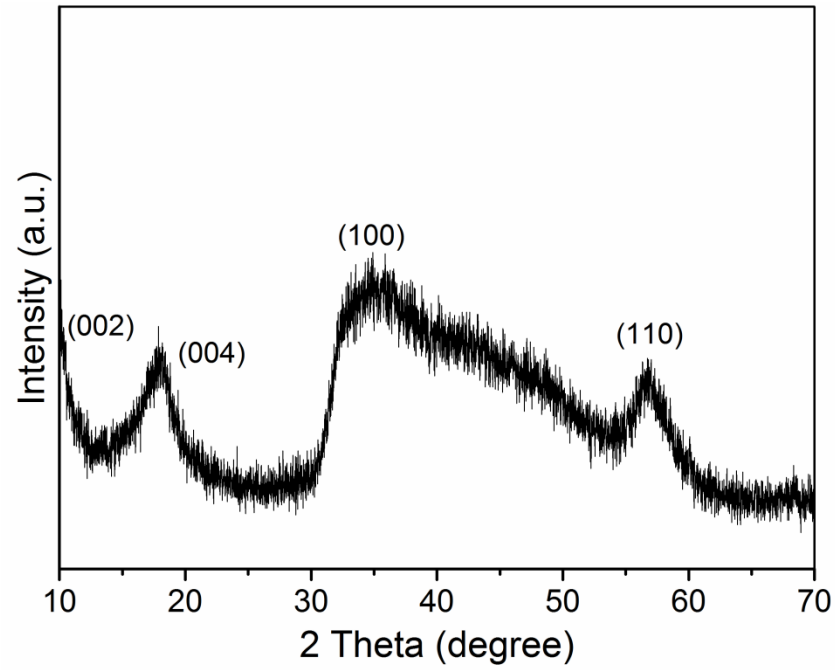

Figure S2. The XRD pattern MoS2 powder.The peak at (002) is significantly shifted compared to the standard card, probably because of a small change in the interlayer spacing.

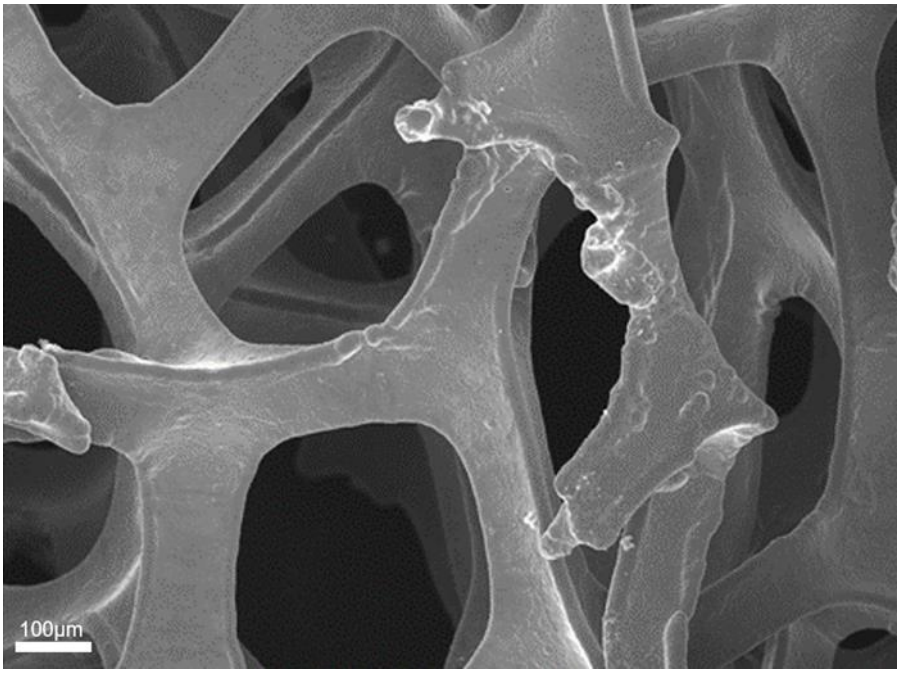

Figure S3. High resolution scanning electron microscopy with NF.

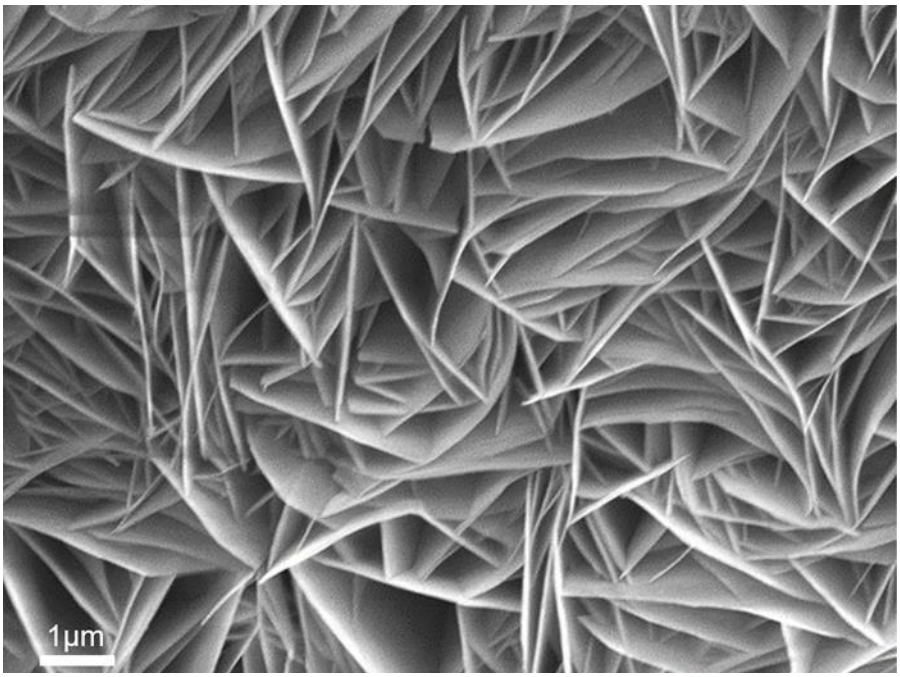

Figure S4. High resolution scanning electron microscopy of $Ni(OH)_2$/NF.

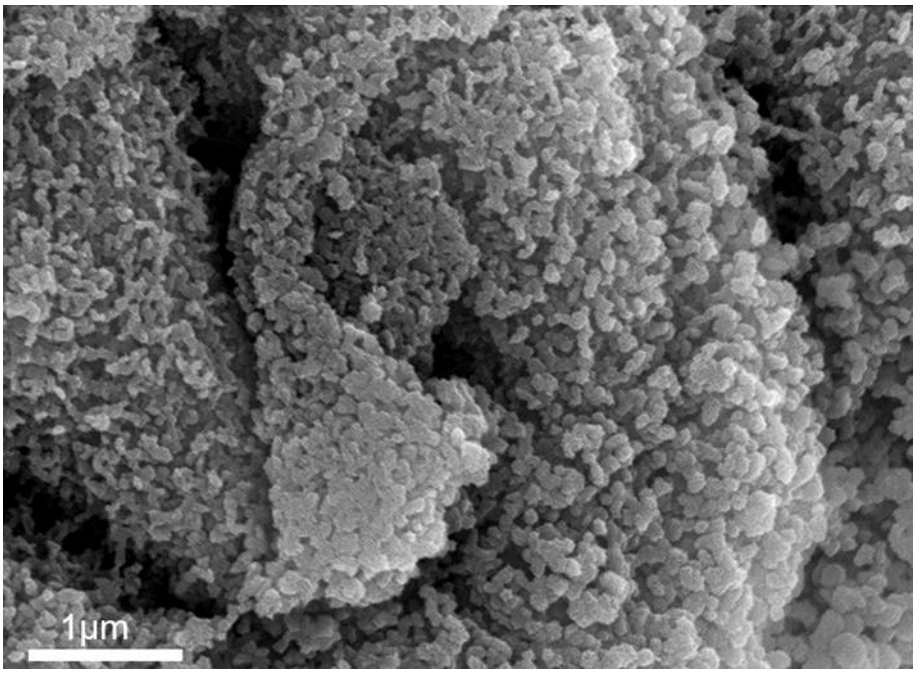

Figure S5. High resolution scanning electron microscopy of MoS_2/NF.

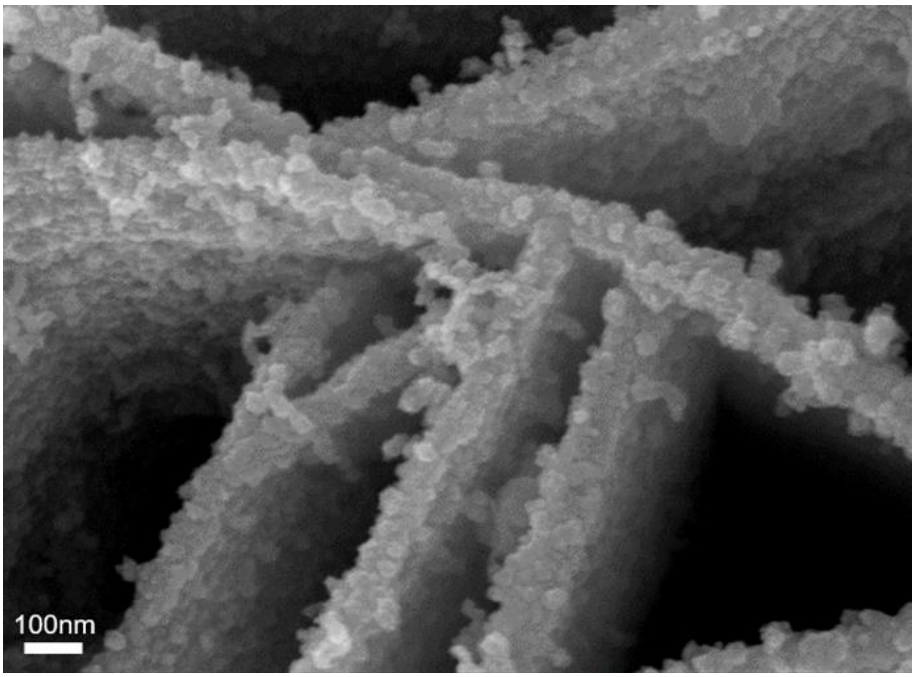

Figure S6. High resolution scanning electron microscopy of $Ni(OH)_2/MoS_2$/NF.

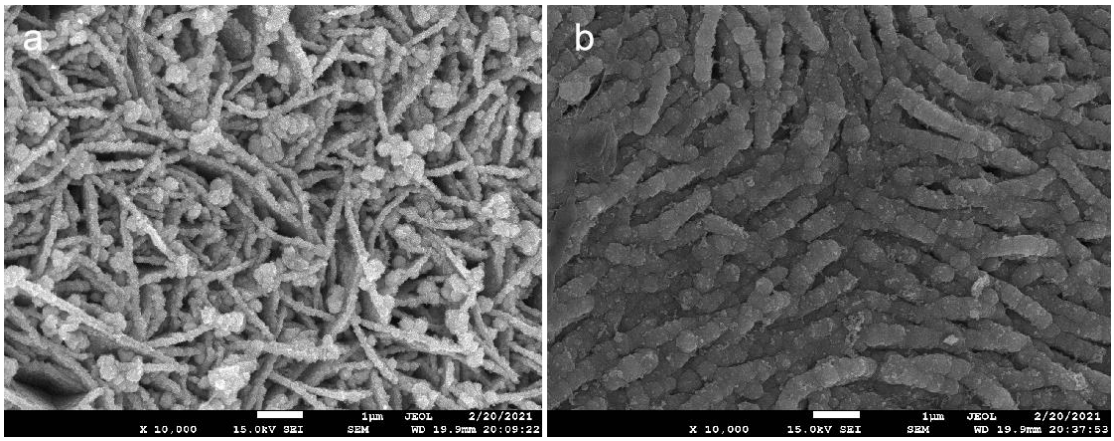

Figure S7. Scanning electron microscopy images of (a)$Ni(OH)_2/MoS_2$/NF-13 and (b) $Ni(OH)_2/MoS_2$/NF-30 electrodes.

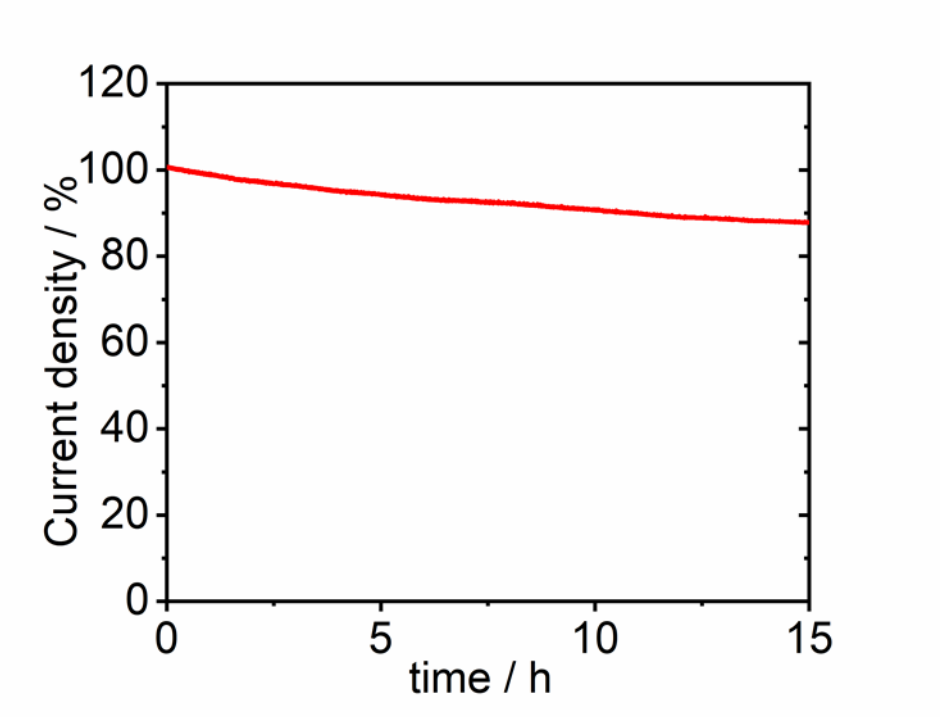

Figure S8. The chronoamperometry measurement of $Ni(OH)_2/MoS_2$/NF electrode.

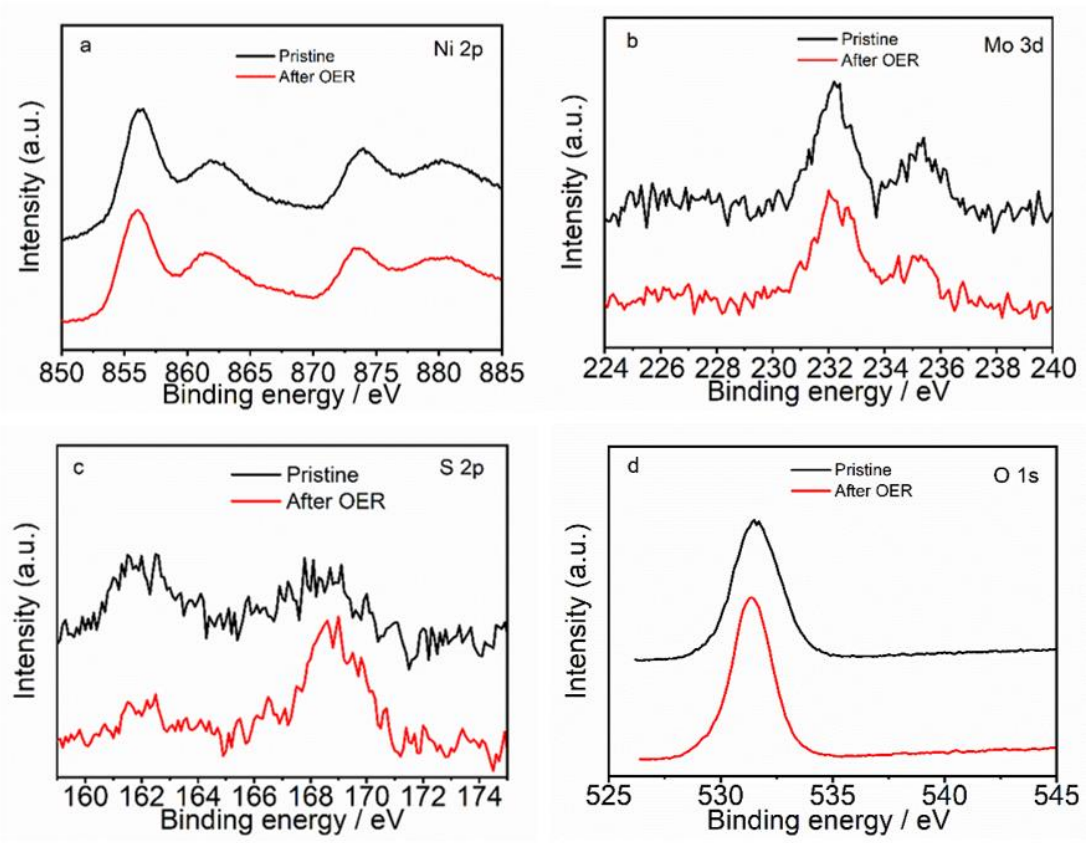

Figure S9. High-resolution XPS (a) Ni 2p, (b) Mo 3d, (c) S 2p and (d) O 1s of $Ni(OH)_2/MoS_2$/NF electrode before and after long- time stability test.

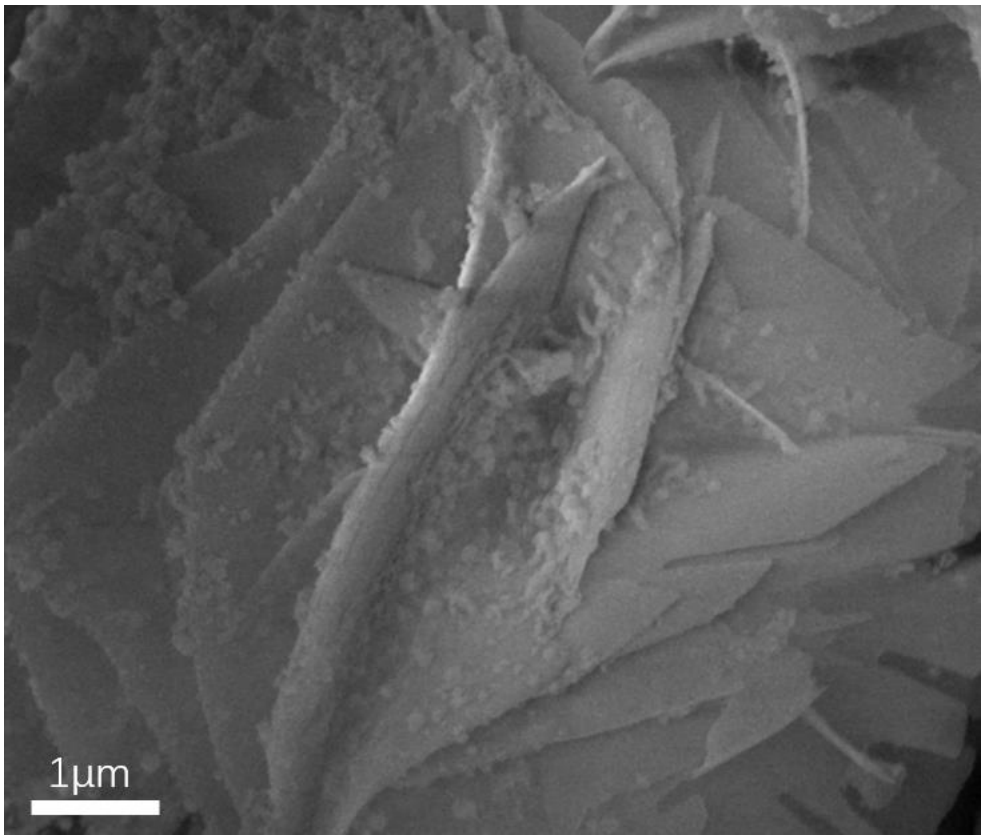

Figure S10. The SEM image of $Ni(OH)_2/MoS_2$/NF electrode after long- time stability test.

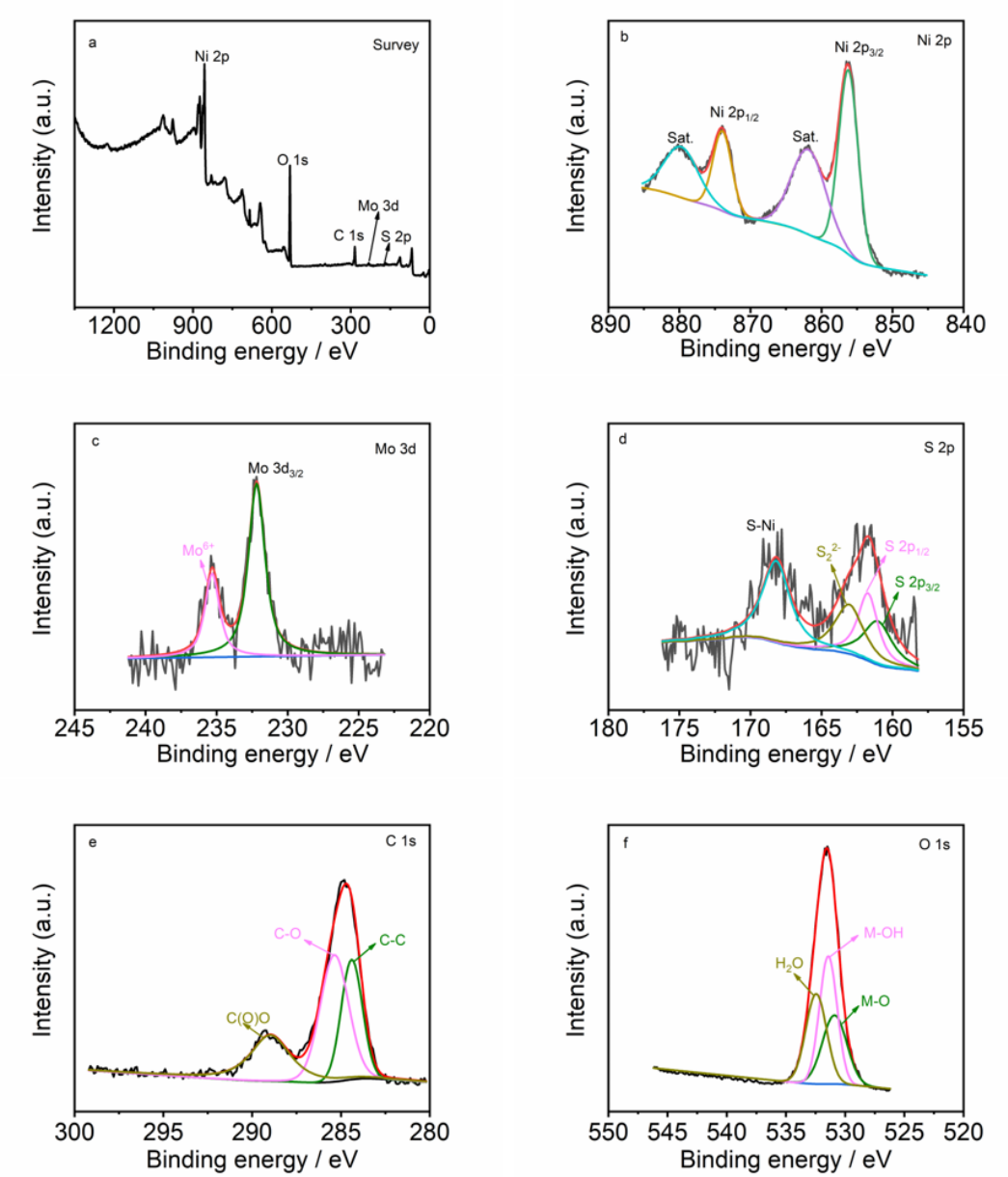

Figure S11. (a) XPS survey spectra, (b) Ni 2p, (c) Mo 3d, (d) S 2p, (e) C 1s and (f) O 1s of $Ni(OH)_2/MoS_2$/NF electrode.

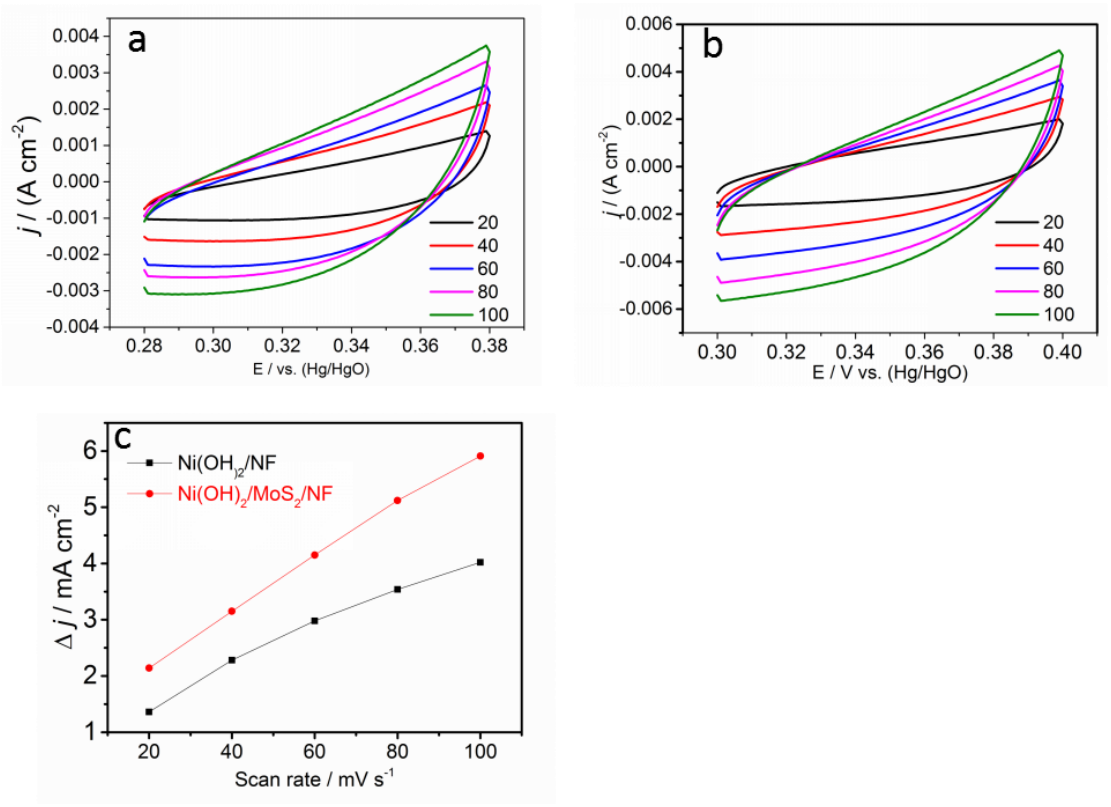

Figure S12. CV curves of the (a) $Ni(OH)_2$/NF and (b) $Ni(OH)_2/MoS_2$/NF electrodes measured at different scan rates from 20 to 100 mV s^{-1} in a potential window without faradaic processes. (c) Plots of the current density vs. the scan rates for $Ni(OH)_2$/NF and $Ni(OH)_2/MoS_2$/NF electrodes.

Table S1. Comparison of OER performance of $Ni(OH)_2/MoS_2$/NF catalyst with other reports

Catalyst	Tafel slope ($mV\ dec^{-1}$)	j($mA\ cm^{-2}$)	Overpotential (η/mV)	Reference
$Ni(OH)_2/MoS_2$/NF	**62**	**50**	**296**	**This work**
		100	**314**	
$Ti@NiCo_2O_4$	61	10	353	International Journal of Hydrogen Energy,2020,46,10259-10267 [1].
$CoMoO_4$	56	10	312	Chem. Commun., 2015, 51, 14361-14364 [2].
CoCr LDH	81	10	340	Mater. Chem. A 2016, 4, 11292-11298 [3].
Co_9S_8 @$Co9S_8@MoS_{2-0.5}$	71.5	10	340	Inorg. Chem. Front., 2020,**7**, 191-197 [4].
$MoS_2@CoO$	129.9	10	325	J. Phys. Chem. C 2019, 123, 10, 5833–5839 [5].
Pd_2/MoS_2	--	10	320	New J. Chem., 2020,44, 16135-16143 [6].
$NiCo_{2.7}(OH)x$	65	10	350	Adv. Energy Mater. 2015,5 ,1401880 [7].
$Co_3O_4/NiCo_2O_4$	88	10	340	J. Am. Chem. Soc. 2015,137, 5590-5595 [8].
Ni/NiO	58	10	470	New J. Chem., 2020,44, 17507-175171 [9]
β -$Co(OH)_2$	57	10	390	ACS Appl. Energy Mater. 2020, 3, 2, 1461-1467 [10].
$Fe_{0.22}Ni_{0.78}(OH)_2$	35	10	315	ACS Appl. Energy Mater.2019,2,3, 1961-1968 [11].
MoS_2 QDs-AC	39	10	370	ACS Catal. 2018, 8, 3, 1683–1689 [12].

References.

1. Bao, W.W.; Xiao, L.; Zhang, J.J.; Jiang, P.; Zou, X.Y.; Yang, C.M.; Hao, X.L.; Ai, T.T. Electronic and structural engineering of $NiCo_2O_4$/Ti electrocatalysts for efficient oxygen evolution reaction, *Int. J. Hydrog. Energy* **2021**, 46, 10259-10267.
2. Yu, M.Q.; Li, X.J.; Hua, G.Y. Ultrathin nanosheets constructed $CoMoO_4$ porous flowers with high activity for electrocatalytic oxygen evolution. *Chem. Commun.* **2015**, 51, 14361-14364.
3. Dong, C.L.; Yuan, X.T.; Wang. X.; Liu, X.Y.; Dong, W.J.; Wang, R.Q.; Duan, Y.H.; Huang, F.Q.; Rational design of cobalt–chromium layered double hydroxide as a highly efficient electrocatalyst for water oxidation, *J. Mater. Chem. A* **2016**, 4, 11292-11298.
4. Li, J.; Li, G.S.; Wang, J.H.; Xue, C.L.; Li, X.S.; Wang, S.; Han, B.Q.; Yang, M.; Li, L.P. A novel core–double shell heterostructure derived from a metal–organic framework for efficient HER, OER and ORR electrocatalysis, *Inorg. Chem. Front.* **2020,** 7, 191-197.
5. Cheng, P.F.; Yuan, C.; Zhou, Q.W.; Hu, X.B.; Li, J.; Lin, X.Z.; Wang, X.; Jin, M.L.; Shui, L.L.; Gao, X.S.; Nötzel, R.; Zhou, G.F.; Zhang, Z.; Liu, J.M. Core–Shell MoS_2@CoO electrocatalyst for water splitting in neural and alkaline solutions, *J. Phys. Chem. C* **2019**, 123, 5833-5839.
6. He, F.; Liu, Y.J.; Ca, Q.H.; Zhao, J.X. Size-dependent electrocatalytic activity of ORR/OER on palladium nanoclusters anchored on defective MoS_2 monolayers, *New J. Chem.* **2020**, 44,16135-16143.
7. Nai, J.W.; Yin, H.J.; You, T.T.; Zheng, L.R.; Zhang, J.; Wang, P.X.; Jin, Z.; Tian, Y.; Liu, J.Z.; Tang, Z.Y.; Guo, L. Efficient electrocatalytic water oxidation by using amorphous Ni–Co double hydroxides nanocages, *Adv. Energy Mater*. **2015**, 5, 1401880.
8. Hu, H.; Guan, B.Y.; Xia, B.Y.; Lou, X.W. Designed formation of Co_3O_4/$NiCo_2O_4$ double-shelled nanocages with enhanced pseudocapacitive and electrocatalytic properties, *J. Am. Chem. Soc.* **2015**, 137, 5590-5595.
9. Paliwala, M.K.; Meher, S.K. Study of "Ni-doping" and "open-pore microstructure" as physico-electrochemical stimuli towards the electrocatalytic efficiency of Ni/NiO for the oxygen evolution reaction, *New J. Chem.* **2020**, 44, 17507-17517.
10. Dileep, N.P.; Vineesh, T.V.; Sarma, P.V.; Chalil, M.V.; Prasad, C.S.; Shaijumon, M.M. Electrochemically Exfoliated β-$Co(OH)_2$ Nanostructures for enhanced oxygen evolution electrocatalysis, *ACS Appl. Energy Mater.* **2020**, 3, 1461-1467.
11. Yan, K.L.; Sheng, M.L.; Sun, X.D.; Song, C.; Cao, Z.; Sun, Y.J. Microwave synthesis of ultrathin nickel hydroxide nanosheets with Iron incorporation for electrocatalytic water oxidation, *ACS Appl. Energy Mater.* **2019**, 2, 1961-1968.
12. Mohanty, B.; Ghorbani-Asl, M.; Kretschmer, S.; Ghosh, A.; Guha, P.; Panda, S.K.; Jena, B.; Krasheninnikov, A.V.; Jena, B.K. MoS_2 quantum dots as efficient catalyst materials for the oxygen evolution reaction, *ACS Catal.* **2018**, 8, 1683-1689.